CD40 and CD80/86 signaling in cDC1s mediate effective neoantigen vaccination and generation of antigen-specific CX3CR1^{+} CD8^{+} T cells in mice

Takayoshi Yamauchi[1,6], Toshifumi Hoki[1,6], Takaaki Oba[1,6], Kristopher Attwood[2], Xuefang Cao[3], and Fumito Ito,[1, 4, 5, *]

[1] Center for Immunotherapy, Roswell Park Comprehensive Cancer Center, Buffalo, NY, USA

[2] Department of Biostatistics and Bioinformatics, Roswell Park Comprehensive Cancer Center, Buffalo, NY 14263, USA

[3] Department of Microbiology and Immunology, University of Maryland School of Medicine, Baltimore MD, USA

[4] Department of Surgical Oncology, Roswell Park Comprehensive Cancer Center, Buffalo, NY, USA

[5] Department of Surgery, Jacobs School of Medicine and Biomedical Sciences, State University of New York at Buffalo, Buffalo, NY 14263, USA

[6] Co-first author

* Corresponding author

Please address all correspondence to F. Ito

Elm and Carlton Streets, Buffalo, NY 14263

Phone: 716-845-1300 FAX: 716-845-1595

Email: fumito.ito@roswellpark.org

Abstract

The use of tumor mutation-derived neoantigen represents a promising approach for cancer vaccines. Preclinical and early-phase human clinical studies have shown the successful induction of tumor neoepitope-directed responses; however, overall clinical efficacy of neoantigen vaccines has been limited. One major obstacle of this strategy is the prevailing lack of sufficient understanding of the mechanism underlying the generation of neoantigen-specific $CD8^+$ T cells. Here, we report a correlation between antitumor efficacy of neoantigen/toll-like receptor 3 (TLR3)/CD40 vaccination and the generation of antigen-specific $CD8^+$ T cells expressing CX3C chemokine receptor 1 (CX3CR1) in a preclinical model. Mechanistic studies using mixed bone marrow chimeras identified that CD40 and CD80/86, but not CD70 signaling in Batf3-dependent conventional type 1 dendritic cells (cDC1s) is required for antitumor efficacy of neoantigen vaccine and generation of neoantigen-specific $CX3CR1^+$ $CD8^+$ T cells. Although $CX3CR1^+$ $CD8^+$ T cells exhibited robust *in vitro* effector function, depletion of this subset did not alter the antitumor efficacy of neoantigen/TLR3/CD40 agonists vaccination, suggesting that the expanded $CX3CR1^+$ $CD8^+$ T cell subset represents the post-differentiated *in vivo* effective CX3CR1-negative $CD8^+$ T cell subset. Taken together, our results reveal a critical role of CD40 and CD80/86 signaling in cDC1s in antitumor efficacy of neoantigen-based therapeutic vaccines, and implicate the potential utility of CX3CR1 as a circulating predictive T-cell biomarker in vaccine therapy.

Key words

Vaccine therapy, Neoantigen, CX3CR1, T cells, Dendritic cells, CD40

45 # Abbreviations

46 Ab: Antibody

47 Batf3: Basic leucine zipper transcription factor ATF-like 3

48 cDC1: Conventional type 1 dendritic cell

49 CTLA-4: Cytotoxic T-lymphocyte-associated protein 4

50 CX3CR1: CX3C chemokine receptor 1

51 DC: Dendritic cell

52 DT: Diphtheria toxin

53 GZMA: Granzyme A

54 HEV: High endothelial venules

55 ICOS: Inducible T cell co-stimulator

56 IFN-γ: Interferon gamma

57 KLRG1: Killer-cell lectin like receptor G1

58 MHC: Major histocompatibility complex

59 NT: No treatment

60 PB: Peripheral blood

61 PD-1: Programmed cell death protein 1

62 poly(I:C): Polyinosinic-polycytidylic acid sodium salt

63 TAM: Tumor associated macrophage

64 TLR3: Toll-like receptor 3

65 TME: Tumor microenvironment

66 TNF-α: Tumor necrosis factor alpha

67 WT: Wild-type

68

69 # Introduction

70 Despite objective therapeutic benefit seen in several clinical trials, the overall clinical
71 success of the peptide-based vaccines has thus far been limited (1, 2). This is due, at least in part,
72 to the low immunogenicity of self-antigens, the incomplete understanding of immunological
73 mechanisms underlying effective priming of tumor-specific T cells, and the lack of a reliable
74 biomarker for clinical response. Somatically mutated genes within tumors can generate
75 neoantigens, which create *de novo* epitopes for T cells (3). Since neoantigens have not undergone
76 central thymic selection, they can be deemed as highly immunogenic tumor-specific antigens (3).
77 Recent advances of neoantigen identification by massive parallel sequencing and computational
78 prediction of neo-epitopes have demonstrated that individualized mutanome-based vaccinations
79 are promising (4-7).

80 The chemokine receptor, CX3CR1, was recently identified as a marker of effector T-cell
81 differentiation (8, 9). Unlike other proliferation, co-stimulatory and co-inhibitory molecules such
82 as Ki67, ICOS, PD-1 and CTLA-4 that are only transiently upregulated on T cells after
83 activation, CX3CR1 is stably expressed on virus- and tumor-specific $CD8^+$ T cells upon
84 differentiation via unidirectional differentiation from the CX3CR1-negative ($CX3CR1^-$) subset
85 during the effector phase (8-10). Furthermore, our study and others have shown that $CD8^+$ T
86 cells expressing high levels of CX3CR1 exhibit decreased expression of L-selectin (CD62L)
87 and CXCR3 (8-10), trafficking receptors necessary for entry across lymphoid organ high
88 endothelial venules (HEV) and the tumor microvasculature, respectively (11, 12), and become
89 more prevalent in peripheral blood (PB) at the end of the primary response (9, 10). These
90 observations prompted us to hypothesize that effective vaccination would be associated with
91 the increased frequency of antigen-specific $CX3CR1^+$ $CD8^+$ T cells in the periphery.

92 Here, we used a syngeneic mouse model of colon adenocarcinoma with the neo-epitope
93 presented in major histocompatibility complex (MHC) class I H-2D^{b} molecules (13), and
94 investigated the relationship between antitumor efficacy of neoantigen vaccination and the
95 frequency of neoantigen-specific CX3CR1^{+} CD8^{+} T cells. Our results indicate that generation of
96 circulating neoantigen-specific CX3CR1^{+} CD8^{+} T cells correlates with successful vaccination
97 with mutated peptide and toll-like receptor 3 (TLR3)/CD40 agonists. Mechanistic studies using
98 mixed bone marrow chimeras identified a key role of CD40 and CD80/86, but not CD70
99 signaling in Batf3-dependent conventional type 1 dendritic cells (cDC1s) for the generation of
100 neoantigen-specific cytotoxic CX3CR1^{+} CD8^{+} T cells and therapeutic efficacy of neoantigen
101 vaccine.

102 # Materials and Methods

103 **Mice**

104 Female C57BL/6 mice were purchased from the Jackson Laboratory. CD40$^{-/-}$ mice
105 (B6.129S2-*Cd40lg*^{tm1Imx}/J), CD80/86$^{-/-}$ mice (B6.129S4-*Cd80*^{tm1Shr} *Cd86*^{tm2Shr}/J), and Batf3$^{-/-}$
106 mice (B6.129S(C)-*Batf3*^{tm1Kmm}/J), CD2-Cre mice (C57BL/6-Tg(CD2-cre)1Lov/J), and CX3CR1-
107 DTR mice (B6N.129P2-Cx3cr1$^{tm3(DTR)Litt}$/J) on C57BL/6 background were purchased from the
108 Jackson Laboratory, and bred in-house (Roswell Park Comprehensive Cancer Center). CD70$^{-/-}$
109 mice on C57BL/6 background have been previously described (14). For inducible *Cd2-*
110 *cre/Cx3cr1*$^{+/DTR}$ mice, we crossed CD2-Cre mice with CX3CR1-DTR mice to generate *Cd2-*
111 *cre/Cx3cr1*$^{+/DTR}$ mice, allowing induction of DTR in CX3CR1^{+} CD8^{+} T cells. For depletion of
112 CX3CR1^{+} CD8^{+} T cells, diphtheria toxin (Sigma) (250 ng/dose/mouse) was administered
113 intraperitoneally (i.p.) every day starting from 1 day before neoantigen vaccination. All mice
114 were 7 to 12 weeks old at the beginning of each experiment, and were maintained under specific
115 pathogen-free conditions at the Roswell Park animal facility according to approved institutional
116 guidelines.

117

118 **Cells**

119 The murine B16F10 melanoma cell line was purchased from ATCC. The MC38 murine
120 colon adenocarcinoma cell line was gift from Dr. Weiping Zou (University of Michigan).
121 B16F10 and MC38 cells were maintained in RPMI (Gibco) supplemented with 10% FBS
122 (Sigma), 1% NEAA (Gibco), 2 mM GlutaMAX-1 (Gibco), 100 U/ml penicillin-streptomycin
123 (Gibco), and 55 μM 2-mercaptoethanol (Gibco). Cells were authenticated by morphology,

124 phenotype and growth, and routinely screened for *Mycoplasma*, and were maintained at 37°C in
125 a humidified 5% CO_2 atmosphere.
126
127 ***In vivo* vaccination and cancer immunotherapy studies**
128 Female C57BL/6 mice were injected s.c. with 5-8 × 10^5 MC38 cells into the right flank.
129 Mice were treated s.c. with 100 µg soluble $Adpgk^{Mut}$ (ASMTNMELM) or AH1 (SPSYVYHQF)
130 peptide (GenScript) with 50 µg poly(I:C) (InvivoGen) and 50 µg agonistic CD40 Ab (BioXCell,
131 clone FGK45) in 100 µl of PBS into the left flank twice 1 week apart. PB, spleen and tumors
132 were harvested for immune monitoring 1 week after the second vaccination. Tumor volumes
133 were calculated by determining the length of short (l) and long (L) diameters (volume = $l^2 \times L/2$).
134 Experimental end points were reached when tumors exceeded 20 mm in diameter or when mice
135 became moribund and showed signs of lateral recumbency, cachexia, lack of response to noxious
136 stimuli, or observable weight loss.
137
138 **Generation of bone marrow chimeras**
139 To generate bone marrow chimeras, C57BL/6 mice were irradiated with 500 cGy
140 followed by a second dose of 550 cGy 3 hours apart. To obtain donor bone marrow, femurs and
141 tibiae were harvested and the bone marrow was flushed out. For $Batf3^{-/-}$/WT, $Batf3^{-/-}$/$CD40^{-/-}$,
142 $Batf3^{-/-}$/CD80/$86^{-/-}$, and $Batf3^{-/-}$/$CD70^{-/-}$ mixed bone marrow chimeras, 5 × 10^6 bone marrow
143 cells of a 1:1 mixture were injected to irradiated C57BL/6 WT mice. After 8-12 weeks,
144 recipients were used for the experiments.
145
146 **Flow cytometry and intracellular granzyme, TNF-α and IFN-γ assay**

147 Fluorochrome-conjugated antibodies are shown in Table S1. DAPI, LIVE/DEAD Fixable
148 Aqua (Thermo Fisher Scientific) staining cells were excluded from analysis. For tetramer
149 staining, PE-labeled MHC class I (H-2D^{b}) specific for mouse Adpgk^{Mut} 299-307
150 (ASMTNMELM) (13) was kindly provided by the NIH Tetramer Core Facility. Detection of
151 intracellular cytokines, granzyme A (GZMA), IFN-γ and TNF-α was performed as described
152 before (10). For intracellular staining of IFN-γ and TNF-α, splenocytes and tumor-infiltrating
153 cells were cocultured with 1 μmol/L of Adpgk^{Mut} or AH1 peptide in the presence of Brefeldin A
154 (BD Biosciences) for 5h *in vitro*. Samples were analyzed using an LSR II or an LSRFortessa
155 (BD Biosciences) with FlowJo software (TreeStar).
156
157 **Statistical Analysis**
158 Continuous measures were compared between two groups using two-tailed t-tests
159 (unpaired and paired) and between multiple groups using one-way ANOVA, with Tukey
160 adjusted post-hoc tests. Survival outcomes were compared using the log-rank test (Mantel-Cox
161 method). Correlations were assessed using the Pearson and Spearman correlation coefficients.
162 Analyses were performed in GraphPad Prism 8.02 (GraphPad Software) and SAS v9.4 (Cary,
163 NC) at a significance level of 0.05.

164 # Results

165 **Vaccination with neoantigen and TLR3/CD40 agonists elicits potent antigen-specific**
166 **antitumor efficacy.**

167 To examine the relationship between antitumor efficacy of neoantigen vaccination and
168 the generation of neoantigen-specific $CD8^+$ T cells, we sought to validate a preclinical model of
169 neoantigen vaccination using MC38 colon adenocarcinoma cells that harbor a single-epitope
170 mutation within the Adpgk protein (**Supplemental Figure 1**) (13). In this model, to maximize
171 the therapeutic efficacy of neoantigen vaccination with mutant Adpgk peptide ($Adpgk^{Mut}$), dual
172 TLR/CD40 stimulation was used as vaccine adjuvants **(Figure 1A**), which has been known to
173 synergistically activate DCs, augment $CD8^+$ T cell expansion, and mediate potent antitumor
174 immunity in multiple preclinical models (14-20). Vaccination of $Adpgk^{Mut}$, but not irrelevant
175 AH1 peptide with agonistic anti-CD40 antibody (Ab), and a TLR3 agonist, poly(I:C) (referred to
176 as $Adpgk^{Mut}$/TLR3/CD40 hereafter) markedly delayed the growth of established MC38 tumors
177 and improved survival **(Figure 1B**). Splenocytes and tumor-infiltrating cells from MC38 tumor-
178 bearing mice treated with $Adpgk^{Mut}$/TLR3/CD40 vaccination contained substantially higher
179 frequency of $CD8^+$ T cells that could produce IFN-γ and TNF-α against $Adpgk^{Mut}$ but not
180 irrelevant AH1 antigen **(Figure 1C** and **Supplemental Figure 2**), suggesting the generation of
181 antigen-specific $CD8^+$ T cells. These findings validate a preclinical model of neoantigen vaccine-
182 based therapy to investigate the role of neoantigen-specific $CD8^+$ T cells.

183

184 **Effective neoantigen/TLR3/CD40 stimulations correlate with generation of antigen-specific**
185 **effector $CX3CR1^+$ $CD8^+$ T cells.**

186 We examined whether effective neoantigen vaccination could generate $CD8^+$ T cells
187 expressing CX3CR1, a marker of effector T-cell differentiation (8, 9). To this end, PB, spleen
188 and tumors were harvested 1 week after second $Adpgk^{Mut}$/TLR3/CD40 vaccination, and
189 CX3CR1 expression was evaluated in $CD8^+$ and neoantigen-specific $CD8^+$ T cells using an
190 $Adpgk^{Mut}$-specific tetramer (Tet) (**Supplementary Figure 3**). $Adpgk^{Mut}$/TLR3/CD40 vaccination
191 substantially increased the frequency of $CD8^+$ and Tet^+ $CD8^+$ T cells expressing CX3CR1 in PB
192 and spleen while the frequency of the $CX3CR1^+$ subset remained unchanged in tumors (**Figure**
193 **2A**).

194 Previous clinical studies showed that functional assessment of T cells such as IFN-γ
195 production and/or cytolytic activity was correlated with response in patients treated with peptide
196 vaccines (21-23). Therefore, we evaluated CX3CR1 expression of T cells expressing effector
197 cytokines, and found that the majority of $CD8^+$ T cells producing effector cytokine against
198 $Adpgk^{Mut}$ were largely positive for CX3CR1 expression (**Supplementary Figure 4A**).
199 Accordingly, frequency of the $CX3CR1^+$ subset in circulating Tet^+ $CD8^+$ T cells correlated with
200 the frequency of $CD8^+$ T cells secreting IFN-γ^+ and TNF-α^+ against $Adpgk^{Mut}$ antigen in spleen
201 (**Supplementary Figure 4B**).

202 Next, we assessed relationship between tumor volume and antigen-specific $CD8^+$ T-cell
203 expansion and differentiation in PB from treated and untreated mice. There was a strong inverse
204 correlation between frequency of circulating $CD8^+$ and Tet^+ $CD8^+$ T cells expressing CX3CR1
205 and tumor volume while the frequency of total Tet^+ $CD8^+$ T cells without CX3CR1 criteria had a
206 moderate inverse correlation with tumor volume **(Figure 2B**).

207 Phenotypical and functional evaluation of circulating $Adpgk^{Mut}$-specific $CX3CR1^-$ and
208 $CX3CR1^+$ subsets revealed that the $CX3CR1^+$ subset contained significantly more 4-$1BB^+$, PD-

209 1^{+}, KLRG^{+} and GZMA^{+} populations (**Figure 2C**), suggesting recently-activated effector T cells.
210 However, CX3CR1^{+} CD8^{+} T cells exhibited decreased expression of trafficking molecules,
211 CD62L and CXCR3, involved in T-cell access into lymphoid tissues and tumor
212 microenvironment (TME), respectively (11, 12), in line with the higher frequency of the
213 CX3CR1^{+} subset in PB in treated mice (**Figure 2A**).
214
215 ***In vivo* antitumor efficacy of antigen-specific CX3CR1^{+} CD8^{+} T cells elicited by**
216 **neoantigen/TLR3/CD40 agonist vaccination.**
217 Previous preclinical studies using CX3CR1$^{-/-}$ mice or CX3CR1 inhibitor suggested a
218 significance of the CX3CR1/CX3CL1 axis in T cell/NK-cell mediated antitumor immunity (24-
219 28). However, CX3CR1 is expressed not only on T and NK cells, but also on monocytes, DCs,
220 monocytic myeloid-derived suppressor cells (M-MDSCs) and tumor-associated macrophages
221 (TAMs) (29, 30), and antitumor efficacy of CX3CR1^{+} CD8^{+} T cells against established tumors
222 remains elusive. Recently, we have reported negligible antitumor efficacy of CX3CR1^{hi} CD8^{+}
223 T cells using a mouse model where tumor antigen-specific CX3CR1^{hi} CD8^{+} T cells can be
224 selectively depleted *in vivo* with diphtheria toxin (DT) (10). Furthermore, adoptive transfer of
225 CX3CR1^{+} CD8^{+} T cells did not affect tumor growth nor survival while the CX3CR1^{-} subset
226 displayed potent antitumor efficacy (10).
227 To elucidate antitumor efficacy of CX3CR1^{+} CD8^{+} T cells elicited by
228 neoantigen/TLR3/CD40 agonists vaccination, we crossed CD2-Cre mice with CX3CR1-DTR
229 mice, and generated *Cd2-cre/Cx3cr1*$^{+/DTR}$ mice. Expression of *Cd2-cre* excises the *loxP*-
230 floxed stop cassette upstream of the DTR-coding region, allowing for DTR expression and
231 CX3CR1^{+} CD8^{+} T cells can be depleted upon administration of DT, with no effect on

232 CX3CR1^{-} CD8^{+} T cells (**Figure 3A, B**). MC38 tumor-bearing *Cd2-cre/Cx3cr1$^{+/DTR}$* mice were
233 treated with Adpgk^{Mut}/TLR3/CD40 vaccination, and received phosphate buffer saline (PBS) or
234 DT injections every day starting 1 day before vaccination (**Figure 3B**). We found that
235 depletion of CX3CR1^{+} CD8^{+} T cells did not alter antitumor efficacy of neoantigen vaccination
236 (**Figure 3C**). This is in line with our recent study using a mouse model of adoptive T-cell
237 therapy (10), suggesting that the expanded CX3CR1^{+} CD8^{+} T cells represent the post-
238 differentiated *in vivo* effective CX3CR1-negative CD8^{+} T cell subset.
239
240 **CD40 signaling is required for antitumor efficacy of neoantigen/TLR3/CD40 agonists and**
241 **generation of antigen-specific CX3CR1^{+} CD8^{+} T cells.**
242 Neoantigen vaccination with a TLR3 agonist increases antigen-specific tumor-infiltrating
243 lymphocytes in a preclinical model (31) and patients (4, 5). CD40 signaling drives robust DC
244 activation to generate cytotoxic CD8^{+} T cells (32, 33), and synergizes with the TLR3 ligand in
245 inducing an expansion of peptide or DC vaccine-primed and adoptively transferred antigen-
246 specific CD8^{+} T cells (14-17). To delineate the role of CD40 signaling in the context of
247 neoantigen vaccination, we examined antitumor efficacy of Adpgk^{Mut}/TLR3/CD40 vaccination
248 and generation of Adpgk^{Mut}-specific CX3CR1^{+} CD8^{+} T cells using CD40$^{-/-}$ mice. Antitumor
249 efficacy of Adpgk^{Mut}/TLR3/CD40 vaccination was abrogated in CD40$^{-/-}$ mice (**Figure 4A**). The
250 lack of increase in the frequency of Adpgk^{Mut}-specific CX3CR1^{+} CD8^{+} T cells in CD40$^{-/-}$ mice
251 denoted the requirement of CD40-CD40 ligand pathway in this process (**Figure 4B**), in line with
252 recent studies showing that CD4^{+} T-cell help or agonistic anti-CD40 Ab facilitates generation of
253 CX3CR1^{+} CD8^{+} T cells (24, 34).
254

255 **A Critical role of CD40 signaling in cDC1s for antitumor efficacy of**
256 **neoantigen/TLR3/CD40 agonists vaccination and generation of antigen-specific CX3CR1^{+}**
257 **CD8^{+} T cells.**

258 Batf3-dependent conventional type 1 dendritic cells (cDC1s) specialize in cross-
259 presentation of exogenous antigens on MHC class I molecules, and play a key role in antitumor
260 immunity and response to immunotherapy (14, 18, 31, 35-37). To assess whether cDC1s are
261 necessary for the generation of CX3CR1^{+} CD8^{+} T cells, we employed mice deficient in Batf3
262 transcription factor and lack cDC1s (35). We found no therapeutic efficacy of
263 Adpgk^{Mut}/TLR3/CD40 vaccination was observed in Batf3$^{-/-}$ mice (**Figure 5A**) along with a
264 significant reduction of CX3CR1^{+} Tet^{+} CD8^{+} T cells (**Figure 5B**), suggesting the requirement of
265 cDC1s for generation of antigen-specific CX3CR1^{+} CD8^{+} T cells.

266 cDC1s express high levels of TLR3, and a TLR3 agonist poly(I:C) has been used in
267 personalized neoantigen vaccine trials with vaccine-related objective responses (5-7). However,
268 the role of CD40 signaling in cDC1s in vaccine-based immunotherapy remains elusive. To
269 address a direct role of CD40 signaling in cDC1 lineage for CX3CR1^{+} CD8^{+} T cell development,
270 we generated CD40$^{-/-}$/Batf3$^{-/-}$ or wild type (WT)/Batf3$^{-/-}$ mixed bone marrow chimeras into
271 irradiated C57BL/6 WT mice. CD40$^{-/-}$/Batf3$^{-/-}$ bone marrow transplanted recipient mice (CD40$^{-/-}$
272 plus Batf3$^{-/-}$ mixed bone marrow chimeras) lack CD40 expression only in Batf3-dependent bone
273 marrow-derived cells while WT/Batf3$^{-/-}$ bone marrow transplanted recipient mice have an intact
274 CD40 signaling. In CD40$^{-/-}$ plus Batf3$^{-/-}$ mixed bone marrow chimeras, CX3CR1^{+} CD8^{+} T-cell
275 responses remained minimal compared to WT plus Batf3$^{-/-}$ mixed bone marrow chimeras,
276 indicating that CD40 expression on cDC1s is pivotal for the CX3CR1^{+} CD8^{+} T-cell induction
277 (**Figure 5C**). In line with these results, mice reconstituted with CD40$^{-/-}$ plus Batf3$^{-/-}$ mixed bone

278 marrow chimeras had substantially decreased antitumor efficacy of Adpgk^{Mut}/TLR3/CD40
279 vaccination compared to mice with WT plus Batf3$^{-/-}$ mixed bone marrow chimeras (**Figure 5D**).
280
281 **Non-redundant requirement of CD80/86 but not CD70 signaling in cDC1s for antitumor**
282 **efficacy of neoantigen/TLR3/CD40 agonists vaccination and generation of antigen-specific**
283 **CX3CR1^{+} CD8^{+} T cells.**
284 In addition to CD40, both CD70 and CD80/86 have been reported to play an important
285 role in DC-mediated T cell activation and persistence (38); however, the role of these molecules
286 on cDC1s for neoantigen-specific T-cell differentiation remains elusive. Therefore, the
287 requirements of CD70 and CD80/86 signaling in cDC1s were assessed in mixed bone marrow
288 chimeric mice of CD70$^{-/-}$ plus Batf3$^{-/-}$ and CD80/86$^{-/-}$ plus Batf3$^{-/-}$. There was no difference in
289 the frequency of Adpgk^{Mut}-specific CX3CR1^{+} CD8^{+} T cells between WT plus Batf3$^{-/-}$ and CD70^{-}
290 $^{/-}$ plus Batf3$^{-/-}$ mixed bone marrow chimeras (**Figure 6A**) with similar tumor control (**Figure 6B**),
291 suggesting a redundant role of CD70 signaling in cDC1s. In sharp contrast, generation of
292 Adpgk^{Mut}-specific CX3CR1^{+} CD8^{+} T cells (**Figure 6C**) and antitumor efficacy of
293 Adpgk^{Mut}/TLR3/CD40 vaccination (**Figure 6D**) were abrogated in the CD80/86$^{-/-}$ plus Batf3$^{-/-}$
294 compared to the control WT plus Batf3$^{-/-}$ mixed bone marrow chimeras. Thus, the CD80/86-
295 CD28 pathway in cDC1s plays a crucial role in mediating antitumor efficacy and generating
296 antigen-specific effector CX3CR1^{+} CD8^{+} T cells in the context of neoantigen vaccination. Taken
297 together, effective neoantigen/TLR3/CD40 agonist vaccination correlates with generation and
298 frequency of circulating antigen-specific CX3CR1^{+} CD8^{+} T cells mediated by CD40 and
299 CD80/86 signaling in cDC1s.
300

301 # Discussion

302 In this study we have shown potent antitumor efficacy of neoantigen/TLR3/CD40
303 stimulations in a preclinical model, and identified a novel link between antitumor efficacy of
304 neoantigen vaccine and an increased frequency of circulating neoantigen-specific CX3CR1^{+}
305 CD8^{+} T cells. Moreover, using mixed bone marrow chimeras from Batf3$^{-/-}$, CD40$^{-/-}$, CD70$^{-/-}$ and
306 CD80/86$^{-/-}$ mice, we have revealed a pivotal role of CD40 and CD80/86 signaling in cDC1s for
307 generation of neoantigen-specific CX3CR1^{+} CD8^{+} T cells and *in vivo* antitumor efficacy of
308 neoantigen/TLR3/CD40 agonists vaccination.

309 Engagement of CD40 on DCs induces costimulatory molecules on their surface,
310 promotes their cytokine production, facilitates the cross-presentation of antigen (32), and
311 synergistically augments expansion of both endogenous and adoptive transferred T cells with
312 TLR agonist (14-19). Our data further demonstrated that among the diversity of the DC subsets
313 cDC1s play a critical role in antitumor efficacy of TLR3/CD40 stimulation. Although poly(I:C)
314 (TLR3 agonist) has been used in neoantigen vaccine clinical studies (5, 6), these findings
315 underscore the implication of agonistic anti-CD40 Ab in combination with poly(I:C) for the
316 maximal engagement of cDC1 in vaccine-based therapy.

317 The molecular and cellular mechanisms underlying differentiation of CX3CR1^{-} to
318 CX3CR1^{+} CD8^{+} T cells remain elusive. Recent studies have indicated that CD4^{+} T-cell help or
319 agonistic anti-CD40 Ab facilitates generation of CX3CR1^{+} CD8^{+} T cells (24, 34). Our results
320 further demonstrated the non-redundant requirement of CD40 signaling in cDC1s for the
321 generation of antigen-specific CX3CR1^{+} CD8^{+} T cells. The observation that CD70 signaling in
322 cDC1s was dispensable for generation of the CX3CR1^{+} subset was unexpected given the several
323 lines of evidence suggesting that CD40 signaling relays the CD4^{+} T-cell help signal by the

324 induction of CD70 expression on DCs (14, 39). However, not all molecules regulated by $CD4^+$
325 T-cell help are mediated by CD27, and cytokine signaling may have contributed to the
326 generation of the $CX3CR1^+$ subset (34). In support of this notion, IL-21 was found to modulate
327 T-cell differentiation and generation of $CX3CR1^+$ $CD8^+$ T cells (24, 40). Additional mechanistic
328 studies are needed to further determine the signaling required for generation of the $CX3CR1^+$
329 subset.

330 The lack of a reliable surrogate marker for clinical response remains the major limitation
331 of vaccine clinical trials (1, 2). Mere presence of vaccine-primed tumor-specific T cells might
332 not correlate with effective regression of the tumor, and cannot be used as a standalone
333 biomarker for vaccine efficacy (41). In our study, although frequency of PB antigen-specific
334 total $CD8^+$ T cells had a positive inverse correlation with tumor volume, differentiation of
335 antigen-specific $CD8^+$ T cells defined by CX3CR1 expression had a markedly higher inverse
336 correlation with tumor volume. Furthermore, our findings of an increased frequency of
337 $CX3CR1^+$ $CD8^+$ T cells that have the ability to produce IFN-γ, TNF-α and GZMA after
338 successful vaccination align with the evidence from previous clinical studies showing that
339 functional assessment of T cells such as IFN-γ production and/or cytolytic activity was
340 correlated with response in patients treated with peptide vaccines (21-23).

341 An increased frequency of the $CX3CR1^+$ subset was identified not only in Tet^+ $CD8^+$ T
342 cells, but also in total $CD8^+$ T cells, which had a strong inverse correlation with tumor volume.
343 It remains unclear, however, whether this was due to an increased frequency of non-specific
344 $CX3CR1^+$ $CD8^+$ T cells or an epitope-spreading phenomenon, the spread of the immune
345 response from one antigen to another antigen expressed in the same tissue (1, 2). Additional
346 studies are required to determine whether $Adpgk^{Mut}$/TLR3/CD40 vaccination-induced

347 CX3CR1^{+} CD8^{+} T cells contain tumor-specific T cells other than Adpgk^{Mut}-specific T cells.
348 Nevertheless, this observation suggests the potential utility of CX3CR1 as a blood-based
349 predictive T-cell biomarker for other immunotherapies such as immune checkpoint inhibitor
350 therapy. Indeed, an increased frequency of PB CX3CR1^{+} CD8^{+} T cells was observed in
351 patients who responded to immune checkpoint inhibitors (28).

352 Our work and others have provided some insights into the theoretical advantages of
353 CX3CR1 as a circulating surrogate marker for vaccine efficacy. Vaccine-primed CX3CR1^{+} CD8^{+}
354 T cells expressed low levels of CD62L and CXCR3, trafficking receptors necessary for entry
355 across lymphoid organ HEV and the tumor microvasculature, respectively (11, 12), that may
356 have contributed to increase its frequency in PB. Furthermore, unlike other T-cell
357 proliferation, activation or co-stimulatory/inhibitory molecules transiently expressed after
358 activation, CX3CR1 is stably expressed on CD8^{+} T cells through unidirectional differentiation
359 from CX3CR1^{-} CD8^{+} T cells during the effector phase (8-10).

360 Although the scope of our study is limited to CX3CR1, another future area of
361 investigation would be to compare the utility of CX3CR1 as a circulating surrogate marker for
362 vaccine efficacy with other molecules such as PD-1, which was reported to be expressed in
363 circulating neoantigen-specific CD8^{+} T cells (42). Notably, our study was limited by the use of a
364 transplantable non-orthotopic mouse tumor model with high mutational burden. Thus, the utility
365 of CX3CR1 as a circulating T-cell biomarker for vaccine therapy targeting endogenous tumor-
366 associated antigens or tumors with lower mutational burden remains uncertain. Further studies in
367 genetically engineered mouse models or mouse tumors harboring endogenous tumor-associated
368 antigen are warranted to better understand the overall utility of CX3CR1 in vaccine therapy.

369 Our *in vivo* depletion study revealed negligible contribution of CX3CR1^{+} CD8^{+} T cells
370 elicited by Adpgk^{Mut}/TLR3/CD40 vaccination against established MC38 tumors, in line with a
371 previous study using a preclinical model of adoptive T cell therapy against B16 melanoma (10).
372 These findings are in parallel to the compelling evidence that terminally-differentiated effector
373 CD8^{+} T cells have less antitumor efficacy *in vivo* compared to less-differentiated T cells (43), but
374 in contrast to previous studies demonstrating decreased antitumor immunity in CX3CR1$^{-/-}$ mice
375 or with the use of the CX3CR1 antagonist (25-28, 34). A possible explanation is that in *Cd2-*
376 *cre/Cx3cr1*$^{+/DTR}$ mice, DT administration does not affect monocytes, DCs, M-MDSCs and
377 TAMs that may express CX3CR1 (29, 30) and negatively regulate antitumor immunity.
378 Another possibility is that CX3CR1/CX3CL1 pathway might not play a significant role in an
379 MC38 tumor model, and trafficking of CX3CR1^{+} CD8^{+} T cells to the TME is not efficient in
380 the setting of their decreased CXCR3 expression (11). Previous preclinical studies using mouse
381 and xenograft tumor models revealed that augmenting CX3CR1/CX3CL1 axis enhances T
382 cell/NK-cell mediated antitumor efficacy (25, 44, 45). Therefore, the role of CX3CR1^{+} CD8^{+} T
383 cells in antitumor reactivity against solid malignancies might be context-dependent, and remains
384 to be elucidated.

385 In summary, our study revealed cDC1-mediated potent antitumor efficacy of neoantigen
386 vaccine with dual TLR3/CD40 stimulation, identified a correlation between antitumor response
387 and the frequency of antigen-specific PB CX3CR1^{+} CD8^{+} T cells, and provided the mechanistic
388 insight into the generation of CX3CR1^{+} CD8^{+} T cells. These data suggest the maximal
389 engagement of cDC1s with TLR3/CD40 stimulation for the development of more effective
390 neoantigen vaccine therapy, and the potential implications of CX3CR1 as a circulating T-cell
391 predictive biomarker for response in future clinical studies.

Acknowledgments

We acknowledge the NIH Tetramer Core Facility (contract HHSN272201300006C) for provision of MHC class I tetramers, Dr. Weiping Zou (University of Michigan, Ann Arbor, Michigan) for MC38 cells, Dr. James J. Moon (University of Michigan, Ann Arbor, Michigan) and Dr. Toshihiro Yokoi (Roswell Park) for technical assistance, and Dr. Suzanne M. Hess and Ms. Judith Epstein for administrative assistance. This work was supported by National Cancer Institute (NCI) grant P30CA016056 involving the use of Roswell Park's Flow and Image Cytometry, Genomic Shared, and Biostatistics & Statistical Genomics Resources. This work was supported by Roswell Park Alliance Foundation and NCI/ K08CA197966 (F. Ito), Uehara Memorial Foundation (T. Oba), and Astellas Foundation for Research on Metabolic Disorders and the Nakatomi Foundation (T. Yamauchi).

Declarations

Funding

This work was supported by Roswell Park Comprehensive Cancer Center and its National Cancer Institute (NCI) award, P30CA016056 involving the use of Roswell Park's Flow and Image Cytometry and Genomic Shared Resources. F.I was supported by Roswell Park Alliance Foundation and NIH/NCI K08CA197966. X.C. was supported by NIH/ R01HL135325. T.Y. was supported by Astellas Foundation for Research on Metabolic Disorders, and the Nakatomi Foundation. T.O. was supported by Uehara Memorial Foundation.

Conflict of interest

The authors declare no conflict of interest.

415

416 **Ethics approval**

417 All animal studies were reviewed and approved by the Roswell Park institutional animal care and
418 use program and facilities (protocol #1316M and 1356M). All aspects of animal research and
419 husbandry were conducted in accordance with the federal Animal Welfare Act and the NIH
420 Guide for the Care and Use of Laboratory Animals.

421

422 **Consent for publication**

423 All author consent for the publication.

424

425 **Availability of data and material**

426 All data generated or analyzed during this study are included in this published article and
427 supplementary information file.

428

429 **Author contributions**

430 T.Y. contributed development of methodology, acquisition of data, analysis and interpretation of
431 data, writing, review, and revision of the manuscript. T.H, contributed development of
432 methodology, acquisition of data, analysis and interpretation of data, review, and revision of the
433 manuscript. T.O. contributed acquisition of data, analysis and interpretation of data, review, and
434 revision of the manuscript. K.A. contributed analysis and interpretation of data, review, and
435 revision of the manuscript. X.C. provided $CD70^{-/-}$ mice, review, and revision of the manuscript.
436 F.I. developed the concept, managed the project, coordinated author activities, and provided final
437 approval of the version to be submitted.

438 # References

439 1. Butterfield LH (2015) Cancer vaccines. BMJ (Clinical research ed.). 350: h988. doi:
440 10.1136/bmj.h988
441 2. Melero I, Gaudernack G, Gerritsen W et al. (2014) Therapeutic vaccines for cancer: an
442 overview of clinical trials. Nature reviews. Clinical oncology. 11: 509-24. doi:
443 10.1038/nrclinonc.2014.111
444 3. Schumacher TN, Schreiber RD (2015) Neoantigens in cancer immunotherapy. Science.
445 348: 69-74. doi: 10.1126/science.aaa4971
446 4. Sahin U, Derhovanessian E, Miller M et al. (2017) Personalized RNA mutanome vaccines
447 mobilize poly-specific therapeutic immunity against cancer. Nature. 547: 222-6. doi:
448 10.1038/nature23003
449 5. Keskin DB, Anandappa AJ, Sun J et al. (2019) Neoantigen vaccine generates intratumoral
450 T cell responses in phase Ib glioblastoma trial. Nature. 565: 234-9. doi: 10.1038/s41586-
451 018-0792-9
452 6. Ott PA, Hu Z, Keskin DB et al. (2017) An immunogenic personal neoantigen vaccine for
453 patients with melanoma. Nature. 547: 217-21. doi: 10.1038/nature22991
454 7. Hilf N, Kuttruff-Coqui S, Frenzel K et al. (2019) Actively personalized vaccination trial for
455 newly diagnosed glioblastoma. Nature. 565: 240-5. doi: 10.1038/s41586-018-0810-y
456 8. Gordon CL, Lee LN, Swadling L et al. (2018) Induction and Maintenance of CX3CR1-
457 Intermediate Peripheral Memory CD8(+) T Cells by Persistent Viruses and Vaccines. Cell
458 Rep. 23: 768-82. doi: 10.1016/j.celrep.2018.03.074
459 9. Gerlach C, Moseman EA, Loughhead SM, Alvarez D, Zwijnenburg AJ, Waanders L, Garg
460 R, de la Torre JC, von Andrian UH (2016) The Chemokine Receptor CX3CR1 Defines

461 Three Antigen-Experienced CD8 T Cell Subsets with Distinct Roles in Immune
462 Surveillance and Homeostasis. Immunity. 45: 1270-84. doi: 10.1016/j.immuni.2016.10.018
463 10. Yamauchi T, Hoki T, Oba T, Saito H, Attwood K, Sabel MS, Chang AE, Odunsi K, Ito F
464 (2020) CX3CR1-CD8+ T cells are critical in antitumor efficacy, but functionally
465 suppressed in the tumor microenvironment. JCI insight. 5: e133920. doi:
466 10.1172/jci.insight.133920
467 11. Mikucki ME, Fisher DT, Matsuzaki J et al. (2015) Non-redundant requirement for CXCR3
468 signalling during tumoricidal T-cell trafficking across tumour vascular checkpoints. Nature
469 communications. 6: 7458. doi: 10.1038/ncomms8458
470 12. von Andrian UH, Mempel TR (2003) Homing and cellular traffic in lymph nodes. Nat Rev
471 Immunol. 3: 867-78. doi: 10.1038/nri1222
472 13. Yadav M, Jhunjhunwala S, Phung QT et al. (2014) Predicting immunogenic tumour
473 mutations by combining mass spectrometry and exome sequencing. Nature. 515: 572-6.
474 doi: 10.1038/nature14001
475 14. Oba T, Hoki T, Yamauchi T, Keler T, Marsh HC, Cao X, Ito F (2020) A Critical Role of
476 CD40 and CD70 Signaling in Conventional Type 1 Dendritic Cells in Expansion and
477 Antitumor Efficacy of Adoptively Transferred Tumor-Specific T Cells. J Immunol. 205:
478 1867-77. doi: 10.4049/jimmunol.2000347
479 15. Nimanong S, Ostroumov D, Wingerath J et al. (2017) CD40 Signaling Drives Potent
480 Cellular Immune Responses in Heterologous Cancer Vaccinations. Cancer research. 77:
481 1918-26. doi: 10.1158/0008-5472.Can-16-2089

482 16. Cho HI, Celis E (2009) Optimized peptide vaccines eliciting extensive CD8 T-cell
483 responses with therapeutic antitumor effects. Cancer research. 69: 9012-9. doi:
484 10.1158/0008-5472.Can-09-2019
485 17. Ahonen CL, Doxsee CL, McGurran SM, Riter TR, Wade WF, Barth RJ, Vasilakos JP,
486 Noelle RJ, Kedl RM (2004) Combined TLR and CD40 triggering induces potent CD8+ T
487 cell expansion with variable dependence on type I IFN. The Journal of experimental
488 medicine. 199: 775-84. doi: 10.1084/jem.20031591
489 18. Oba T, Long MD, Keler T, Marsh HC, Minderman H, Abrams SI, Liu S, Ito F (2020)
490 Overcoming primary and acquired resistance to anti-PD-L1 therapy by induction and
491 activation of tumor-residing cDC1s. Nature communications. 11: 5415. doi:
492 10.1038/s41467-020-19192-z
493 19. Scarlett UK, Cubillos-Ruiz JR, Nesbeth YC, Martinez DG, Engle X, Gewirtz AT, Ahonen
494 CL, Conejo-Garcia JR (2009) In situ stimulation of CD40 and Toll-like receptor 3
495 transforms ovarian cancer-infiltrating dendritic cells from immunosuppressive to
496 immunostimulatory cells. Cancer research. 69: 7329-37. doi: 10.1158/0008-5472.Can-09-
497 0835
498 20. Khalil DN, Suek N, Campesato LF et al. (2019) In situ vaccination with defined factors
499 overcomes T cell exhaustion in distant tumors. J Clin Invest. 129: 3435-47. doi:
500 10.1172/jci128562
501 21. Carbone DP, Ciernik IF, Kelley MJ et al. (2005) Immunization with mutant p53- and K-
502 ras-derived peptides in cancer patients: immune response and clinical outcome. J Clin
503 Oncol. 23: 5099-107. doi: 10.1200/jco.2005.03.158

504 22. Kirkwood JM, Lee S, Moschos SJ, Albertini MR, Michalak JC, Sander C, Whiteside T,
505 Butterfield LH, Weiner L (2009) Immunogenicity and antitumor effects of vaccination with
506 peptide vaccine+/-granulocyte-monocyte colony-stimulating factor and/or IFN-alpha2b in
507 advanced metastatic melanoma: Eastern Cooperative Oncology Group Phase II Trial E1696.
508 Clin Cancer Res. 15: 1443-51. doi: 10.1158/1078-0432.Ccr-08-1231
509 23. Dillon PM, Olson WC, Czarkowski A, Petroni GR, Smolkin M, Grosh WW, Chianese-
510 Bullock KA, Deacon DH, Slingluff CL, Jr. (2014) A melanoma helper peptide vaccine
511 increases Th1 cytokine production by leukocytes in peripheral blood and immunized lymph
512 nodes. Journal for immunotherapy of cancer. 2: 23. doi: 10.1186/2051-1426-2-23
513 24. Zander R, Schauder D, Xin G, Nguyen C, Wu X, Zajac A, Cui W (2019) CD4(+) T Cell
514 Help Is Required for the Formation of a Cytolytic CD8(+) T Cell Subset that Protects
515 against Chronic Infection and Cancer. Immunity. 51: 1028-42.e4. doi:
516 10.1016/j.immuni.2019.10.009
517 25. Xin H, Kikuchi T, Andarini S et al. (2005) Antitumor immune response by CX3CL1
518 fractalkine gene transfer depends on both NK and T cells. Eur J Immunol. 35: 1371-80.
519 doi: 10.1002/eji.200526042
520 26. Zeng Y, Huebener N, Fest S et al. (2007) Fractalkine (CX3CL1)- and interleukin-2-
521 enriched neuroblastoma microenvironment induces eradication of metastases mediated by
522 T cells and natural killer cells. Cancer research. 67: 2331-8. doi: 10.1158/0008-5472.Can-
523 06-3041
524 27. Yu YR, Fong AM, Combadiere C, Gao JL, Murphy PM, Patel DD (2007) Defective
525 antitumor responses in CX3CR1-deficient mice. Int J Cancer. 121: 316-22. doi:
526 10.1002/ijc.22660

527 28. Yan Y, Cao S, Liu X et al. (2018) CX3CR1 identifies PD-1 therapy-responsive CD8+ T
528 cells that withstand chemotherapy during cancer chemoimmunotherapy. JCI insight. 3:
529 e97828. doi: 10.1172/jci.insight.97828
530 29. Nishimura M, Umehara H, Nakayama T, Yoneda O, Hieshima K, Kakizaki M, Dohmae N,
531 Yoshie O, Imai T (2002) Dual functions of fractalkine/CX3C ligand 1 in trafficking of
532 perforin+/granzyme B+ cytotoxic effector lymphocytes that are defined by CX3CR1
533 expression. J Immunol. 168: 6173-80.
534 30. Bronte V, Brandau S, Chen SH et al. (2016) Recommendations for myeloid-derived
535 suppressor cell nomenclature and characterization standards. Nature communications. 7:
536 12150. doi: 10.1038/ncomms12150
537 31. Sanchez-Paulete AR, Cueto FJ, Martinez-Lopez M et al. (2016) Cancer Immunotherapy
538 with Immunomodulatory Anti-CD137 and Anti-PD-1 Monoclonal Antibodies Requires
539 BATF3-Dependent Dendritic Cells. Cancer Discov. 6: 71-9. doi: 10.1158/2159-8290.cd-
540 15-0510
541 32. Elgueta R, Benson MJ, de Vries VC, Wasiuk A, Guo Y, Noelle RJ (2009) Molecular
542 mechanism and function of CD40/CD40L engagement in the immune system. Immunol
543 Rev. 229: 152-72. doi: 10.1111/j.1600-065X.2009.00782.x
544 33. Vonderheide RH (2018) The Immune Revolution: A Case for Priming, Not Checkpoint.
545 Cancer Cell. 33: 563-9. doi: 10.1016/j.ccell.2018.03.008
546 34. Ahrends T, Spanjaard A, Pilzecker B, Babala N, Bovens A, Xiao Y, Jacobs H, Borst J
547 (2017) CD4(+) T Cell Help Confers a Cytotoxic T Cell Effector Program Including
548 Coinhibitory Receptor Downregulation and Increased Tissue Invasiveness. Immunity. 47:
549 848-61.e5. doi: 10.1016/j.immuni.2017.10.009

550 35. Hildner K, Edelson BT, Purtha WE et al. (2008) Batf3 deficiency reveals a critical role for
551 CD8alpha+ dendritic cells in cytotoxic T cell immunity. Science. 322: 1097-100. doi:
552 10.1126/science.1164206
553 36. Broz ML, Binnewies M, Boldajipour B et al. (2014) Dissecting the tumor myeloid
554 compartment reveals rare activating antigen-presenting cells critical for T cell immunity.
555 Cancer Cell. 26: 638-52. doi: 10.1016/j.ccell.2014.09.007
556 37. Morrison AH, Diamond MS, Hay CA, Byrne KT, Vonderheide RH (2020) Sufficiency of
557 CD40 activation and immune checkpoint blockade for T cell priming and tumor immunity.
558 Proc Natl Acad Sci U S A. 117: 8022-31. doi: 10.1073/pnas.1918971117
559 38. Bak SP, Barnkob MS, Bai A, Higham EM, Wittrup KD, Chen J (2012) Differential
560 requirement for CD70 and CD80/CD86 in dendritic cell-mediated activation of tumor-
561 tolerized CD8 T cells. J Immunol. 189: 1708-16. doi: 10.4049/jimmunol.1201271
562 39. Borst J, Ahrends T, Babala N, Melief CJM, Kastenmuller W (2018) CD4(+) T cell help in
563 cancer immunology and immunotherapy. Nat Rev Immunol. 18: 635-47. doi:
564 10.1038/s41577-018-0044-0
565 40. Tian Y, Cox MA, Kahan SM, Ingram JT, Bakshi RK, Zajac AJ (2016) A Context-
566 Dependent Role for IL-21 in Modulating the Differentiation, Distribution, and Abundance
567 of Effector and Memory CD8 T Cell Subsets. J Immunol. 196: 2153-66. doi:
568 10.4049/jimmunol.1401236
569 41. Rosenberg SA, Sherry RM, Morton KE et al. (2005) Tumor progression can occur despite
570 the induction of very high levels of self/tumor antigen-specific CD8+ T cells in patients
571 with melanoma. J Immunol. 175: 6169-76.

572 42. Gros A, Parkhurst MR, Tran E et al. (2016) Prospective identification of neoantigen-
573 specific lymphocytes in the peripheral blood of melanoma patients. Nat Med. 22: 433-8.
574 doi: 10.1038/nm.4051
575 43. Restifo NP, Dudley ME, Rosenberg SA (2012) Adoptive immunotherapy for cancer:
576 harnessing the T cell response. Nat Rev Immunol. 12: 269-81. doi: 10.1038/nri3191
577 nri3191 [pii]
578 44. Guo J, Zhang M, Wang B, Yuan Z, Guo Z, Chen T, Yu Y, Qin Z, Cao X (2003) Fractalkine
579 transgene induces T-cell-dependent antitumor immunity through chemoattraction and
580 activation of dendritic cells. Int J Cancer. 103: 212-20. doi: 10.1002/ijc.10816
581 45. Siddiqui I, Erreni M, van Brakel M, Debets R, Allavena P (2016) Enhanced recruitment of
582 genetically modified CX3CR1-positive human T cells into Fractalkine/CX3CL1 expressing
583 tumors: importance of the chemokine gradient. Journal for immunotherapy of cancer. 4: 21.
584 doi: 10.1186/s40425-016-0125-1
585

Figure 1

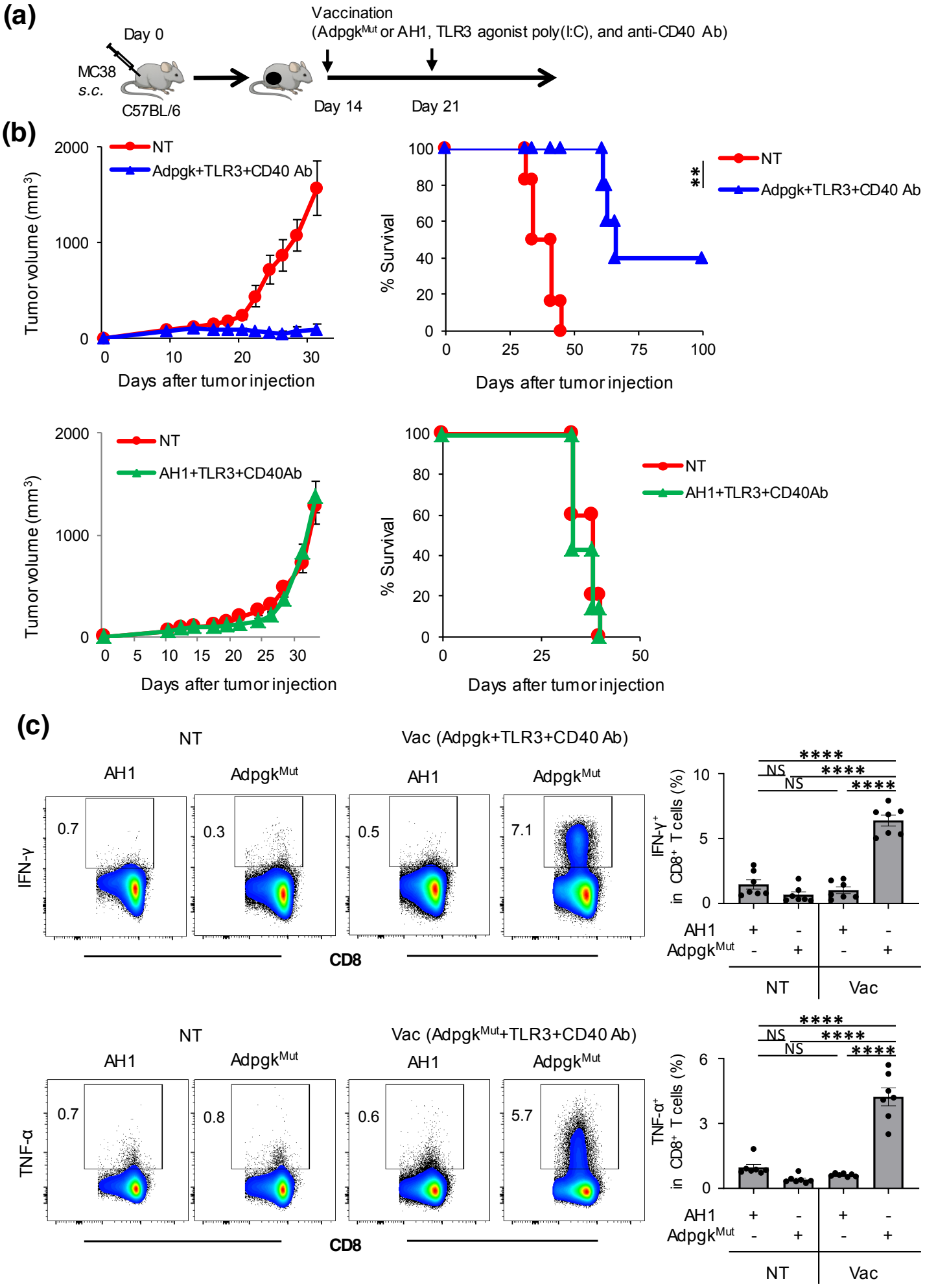
(a)
Day 0
MC38
s.c.
C57BL/6
Vaccination
(Adpgk^Mut or AH1, TLR3 agonist poly(I:C), and anti-CD40 Ab)
Day 14
Day 21
(b)
NT
Adpgk+TLR3+CD40 Ab
Tumor volume (mm³)
Days after tumor injection
% Survival
**
AH1+TLR3+CD40Ab
(c)
NT
Vac (Adpgk+TLR3+CD40 Ab)
AH1
Adpgk^Mut
IFN-γ
CD8
0.7
0.3
0.5
7.1
IFN-γ⁺ in CD8⁺ T cells (%)
NS
****
Vac (Adpgk^Mut+TLR3+CD40 Ab)
TNF-α
0.8
0.6
5.7
TNF-α⁺ in CD8⁺ T cells (%)

Figure 1. Vaccination with neoantigen and TLR3/CD40 agonists elicits potent antigen-specific antitumor efficacy.

(**a**) Experimental scheme for evaluation of neoantigen/TLR3/CD40 agonists vaccination (Vac) in an MC38 tumor model (refer Materials and Methods for details).

(**b**) Tumor growth and survival curves in MC38 tumor-bearing C57BL/6 mice treated with PBS (NT: non-treatment) or $Adpgk^{Mut}$/TLR3/CD40 agonists vaccination (upper) (n = 6 mice per group) and PBS (NT) or AH1/TLR3/CD40 agonists vaccination (lower) (n = 5-7 mice per group).

(**c**) Left shows representative FACS plots showing CD8 and IFN-γ (upper) or TNF-α (lower) expression gated with $CD8^+$ T cells in splenocytes of MC38-tumor bearing mice 1 week after second PBS injection (NT) or $Adpgk^{Mut}$/TLR3/CD40 agonists vaccination. Splenocytes were co-cultured with $Adpgk^{Mut}$ or AH1 peptide in the presence of Brefeldin A for 5 hrs before intracellular staining. Numbers denote percentage of IFN-γ^+ or TNF-α^+ cells. Right panel shows the frequency of the IFN-γ^+ or TNF-α^+ cells in $CD8^+$ T cells in each group (n = 7 mice per group). NS not significant, ****$P < 0.0001$ by log-rank (Mantel-Cox) test (**b**) and one-way ANOVA with Tukey's multiple comparisons (**c**). Mean ± SEM.

Figure 2

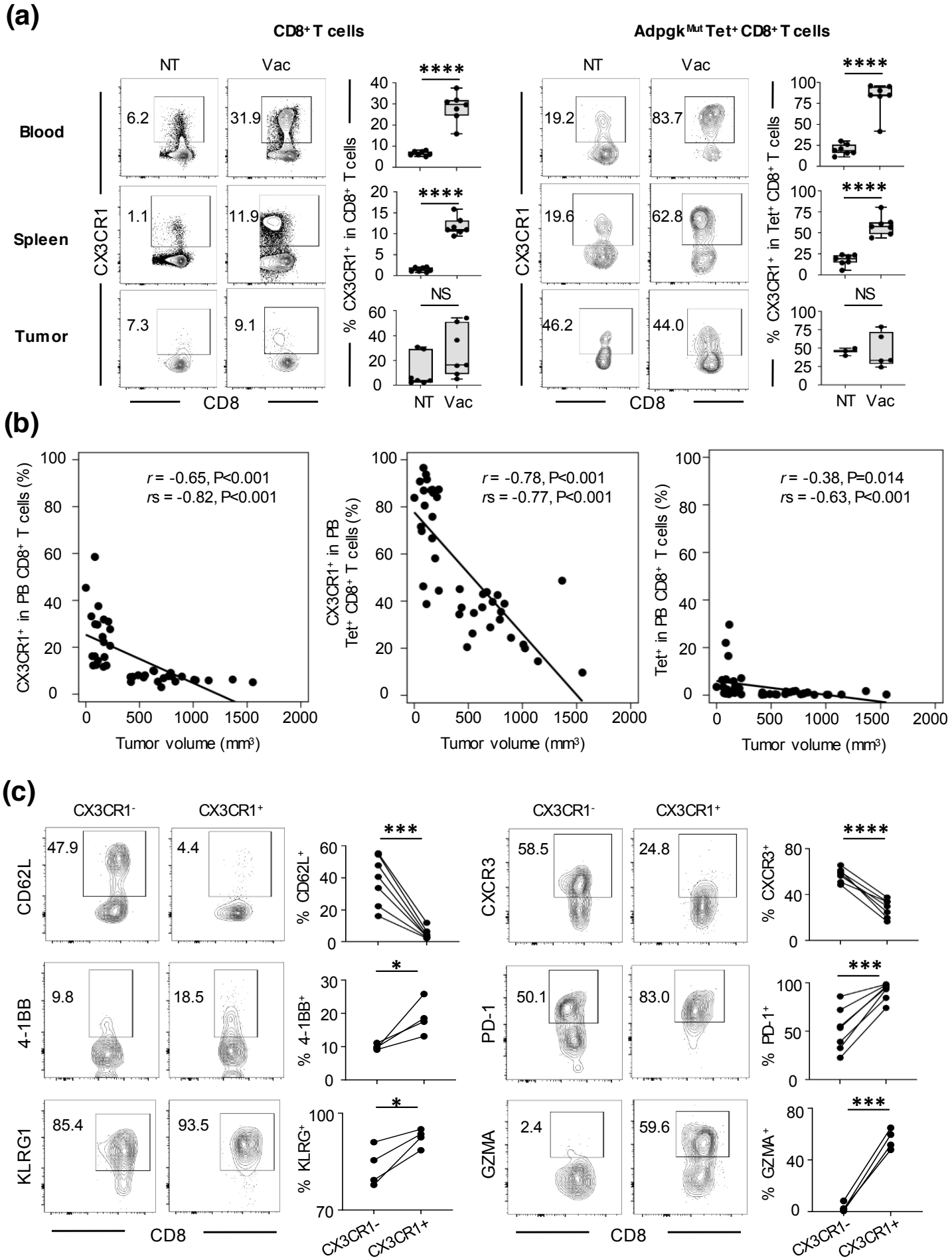
(a)
CD8+ T cells
Adpgk Mut Tet+ CD8+ T cells
NT
Vac
Blood
Spleen
Tumor
CX3CR1
CD8
6.2
31.9
1.1
11.9
7.3
9.1
19.2
83.7
19.6
62.8
46.2
44.0
% CX3CR1+ in CD8+ T cells
% CX3CR1+ in Tet+ CD8+ T cells
****
NS
(b)
CX3CR1+ in PB CD8+ T cells (%)
CX3CR1+ in PB Tet+ CD8+ T cells (%)
Tet+ in PB CD8+ T cells (%)
Tumor volume (mm3)
r = -0.65, P<0.001
rs = -0.82, P<0.001
r = -0.78, P<0.001
rs = -0.77, P<0.001
r = -0.38, P=0.014
rs = -0.63, P<0.001
(c)
CX3CR1-
CX3CR1+
CD62L
4-1BB
KLRG1
CXCR3
PD-1
GZMA
47.9
4.4
9.8
18.5
85.4
93.5
58.5
24.8
50.1
83.0
2.4
59.6
% CD62L+
% 4-1BB+
% KLRG+
% CXCR3+
% PD-1+
% GZMA+
***
*

Figure 2. Effective neoantigen/TLR3/CD40 stimulations correlate with generation of antigen-specific effector CX3CR1^{+}CD8^{+} T cells.

(**a**) Representative FACS plots showing CX3CR1 expression in CD8^{+} (left) or Adpgk^{Mut} tetramer (Tet)$^{+}$CD8^{+} T cells (right) in peripheral blood (PB) (upper), spleen (middle) and tumors (lower) from MC38-tumor bearing mice 1 week after second Adpgk^{Mut}/TLR3/CD40 agonists vaccination (Vac). Numbers denote percentage of CX3CR1-positive cells. Frequency of CX3CR1-positive cells from the CD8^{+} or Tet^{+}CD8^{+} T cells is shown in the right panels (n = 3-7 mice per group). Data shown are representative of three independent experiments.

(**b**) Scatter plot of the frequency of PB CX3CR1^{+}CD8^{+} (left), CX3CR1^{+}Tet^{+}CD8^{+} T cells (middle), and Tet^{+}CD8^{+} T cells against tumor volume in untreated and treated mice 1 week after second Adpgk^{Mut}/TLR3/CD40 agonists vaccination. Correlation is shown using Pearson correlation (r) and Spearman correlation coefficients (r_s). Data shown are representative of two independent experiments.

(**c**) Representative FACS plots of CX3CR1^{-} (left) or CX3CR1^{+} (right) cells gated with Tet^{+}CD8^{+} T cells in PB of MC38-tumor bearing mice 1 week after second Adpgk^{Mut}/TLR3/CD40 agonists vaccination. Numbers denote percentage of each marker-positive cells. Frequency of marker-positive cells from the CX3CR1^{-} or CX3CR1^{+} subset is shown in the right panels for each marker (n = 4-7 mice per group). Data shown are representative of two independent experiments. NS: not significant, $*P < 0.05$, $***P < 0.001$, $****P < 0.0001$ by unpaired (**a**) and paired two-tailed t-test (**c**). Mean ± SEM.

Figure 3

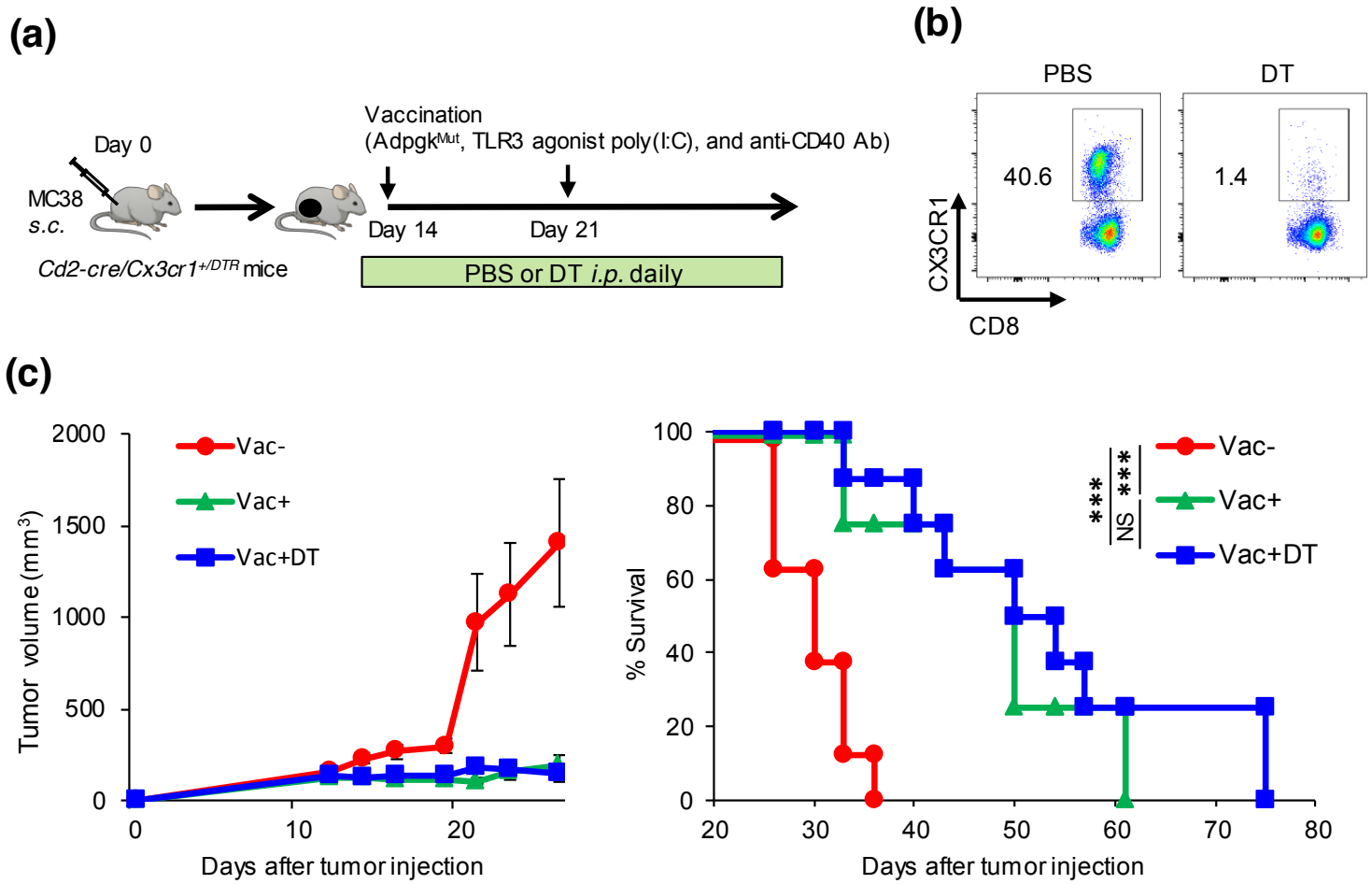
(a)
Day 0
MC38
s.c.
Cd2-cre/Cx3cr1+/DTR mice
Vaccination
(AdpgkMut, TLR3 agonist poly(I:C), and anti-CD40 Ab)
Day 14
Day 21
PBS or DT i.p. daily
(b)
PBS
DT
40.6
1.4
CX3CR1
CD8
(c)
Vac-
Vac+
Vac+DT
Tumor volume (mm3)
Days after tumor injection
% Survival
Days after tumor injection
***
***
NS

Figure 3. *In vivo* antitumor efficacy of antigen-specific CX3CR1^{+}CD8^{+} T cells elicited by neoantigen/TLR3/CD40 agonists vaccination.

(**a**) Schematic illustration showing evaluation of *in vivo* antitumor efficacy of the CX3CR1^{+} subset using MC38 tumor-bearing *Cd2-cre/Cx3cr1*$^{+/DTR}$ mice treated with Adpgk^{Mut}/TLR3/CD40 agonists vaccination (Vac) followed by diphtheria toxin (DT) administration. DT (250 ng) was injected intraperitoneally every day from day 13.

(**b**) Representative FACS plots showing selective depletion of CX3CR1^{+} subset in PB upon DT injection in *Cd2-cre/Cx3cr1*$^{+/DTR}$ mice treated with Vac. Expression of CX3CR1 in CD8^{+} T cells in peripheral blood of mice treated with PBS or DT are shown. Numbers denote percentage of the CX3CR1^{+} subset.

(**c**) Tumor growth and survival curves of MC38 tumor-bearing *Cd2-cre/Cx3cr1*$^{+/DTR}$ mice in different treatment groups. ($n \geq 7$ mice per group). Data shown are representative of two independent experiments.

Data shown are representative from two independent experiments. ***$P < 0.001$, ****$P < 0.0001$ by log-rank (Mantel-Cox) test (**c**) or paired two-tailed *t*-test (**d**). Mean ± SEM.

Figure 4

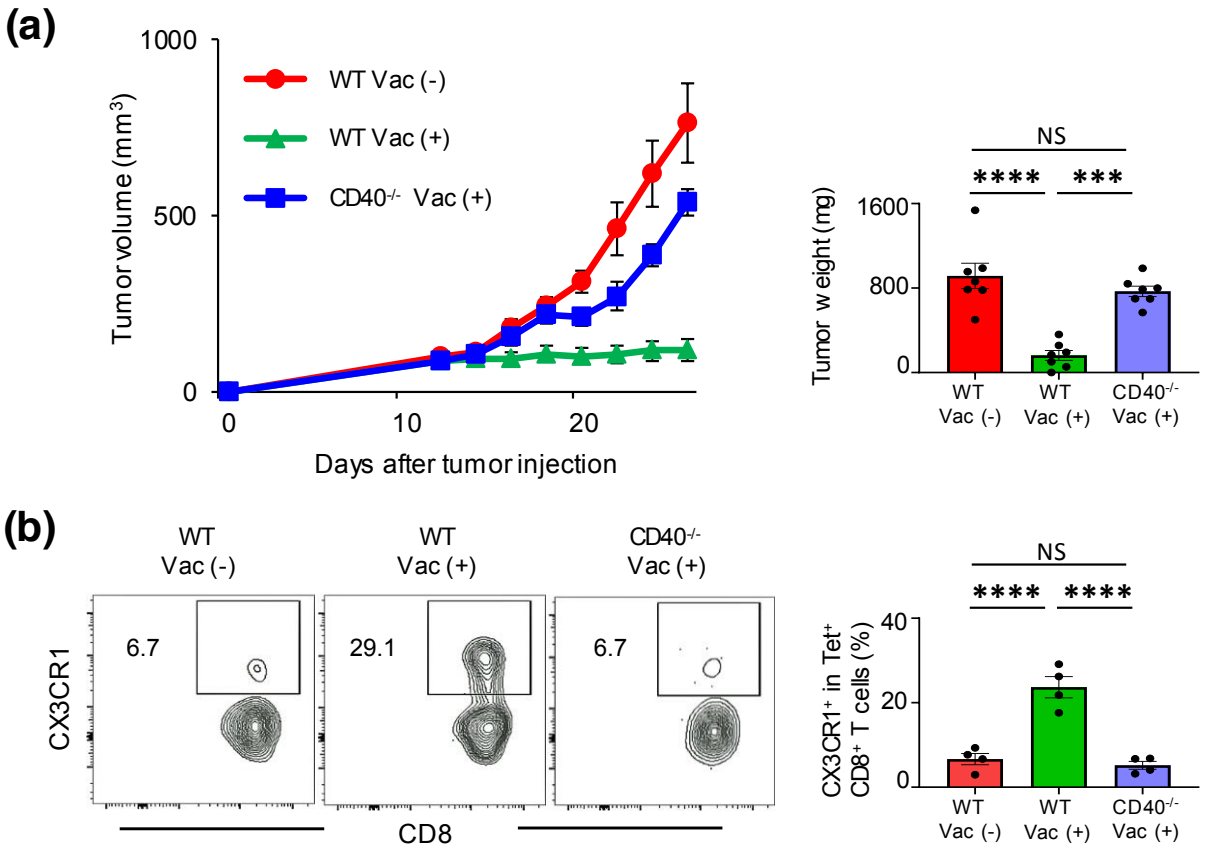
(a)
1000
500
0
Tumor volume (mm3)
WT Vac (-)
WT Vac (+)
CD40-/- Vac (+)
0
10
20
Days after tumor injection
NS
****
***
1600
800
0
Tumor weight (mg)
WT Vac (-)
WT Vac (+)
CD40-/- Vac (+)
(b)
WT Vac (-)
WT Vac (+)
CD40-/- Vac (+)
CX3CR1
6.7
29.1
6.7
CD8
NS
****
****
40
20
0
CX3CR1+ in Tet+ CD8+ T cells (%)
WT Vac (-)
WT Vac (+)
CD40-/- Vac (+)

Figure 4. CD40-dependent generation of antigen-specific CX3CR1^{+}CD8^{+} T-cell subsets upon neoantigen/TLR3/CD40 agonists vaccination.

(**a**) Left shows tumor volume curves in MC38 tumor-bearing wild type C57BL/6 mice (WT) or CD40$^{-/-}$ mice treated with or without Adpgk^{Mut}/TLR3/CD40 agonists vaccination (Vac) (n = 7 mice per group). Right shows tumor weight. Tumors were harvested 1 week after second vaccination (Vac).

(**b**) Left shows representative FACS plots showing CD8 and CX3CR1 expression gated with Adpgk^{Mut} Tet^{+}CD8^{+} T cells in peripheral blood (PB) of MC38-tumor bearing WT or CD40$^{-/-}$ mice treated with or without Vac. Numbers denote percentage of the CX3CR1^{+} subset. Right shows the frequency of the CX3CR1^{+} subset in each group (n = 4 mice per group). PB was harvested 1 week after second Vac. Data shown are representative of two independent experiments. NS: not significant, ***P <0.001, ****P <0.0001 by one-way ANOVA with Tukey's multiple comparisons. Mean ± SEM.

Figure 5

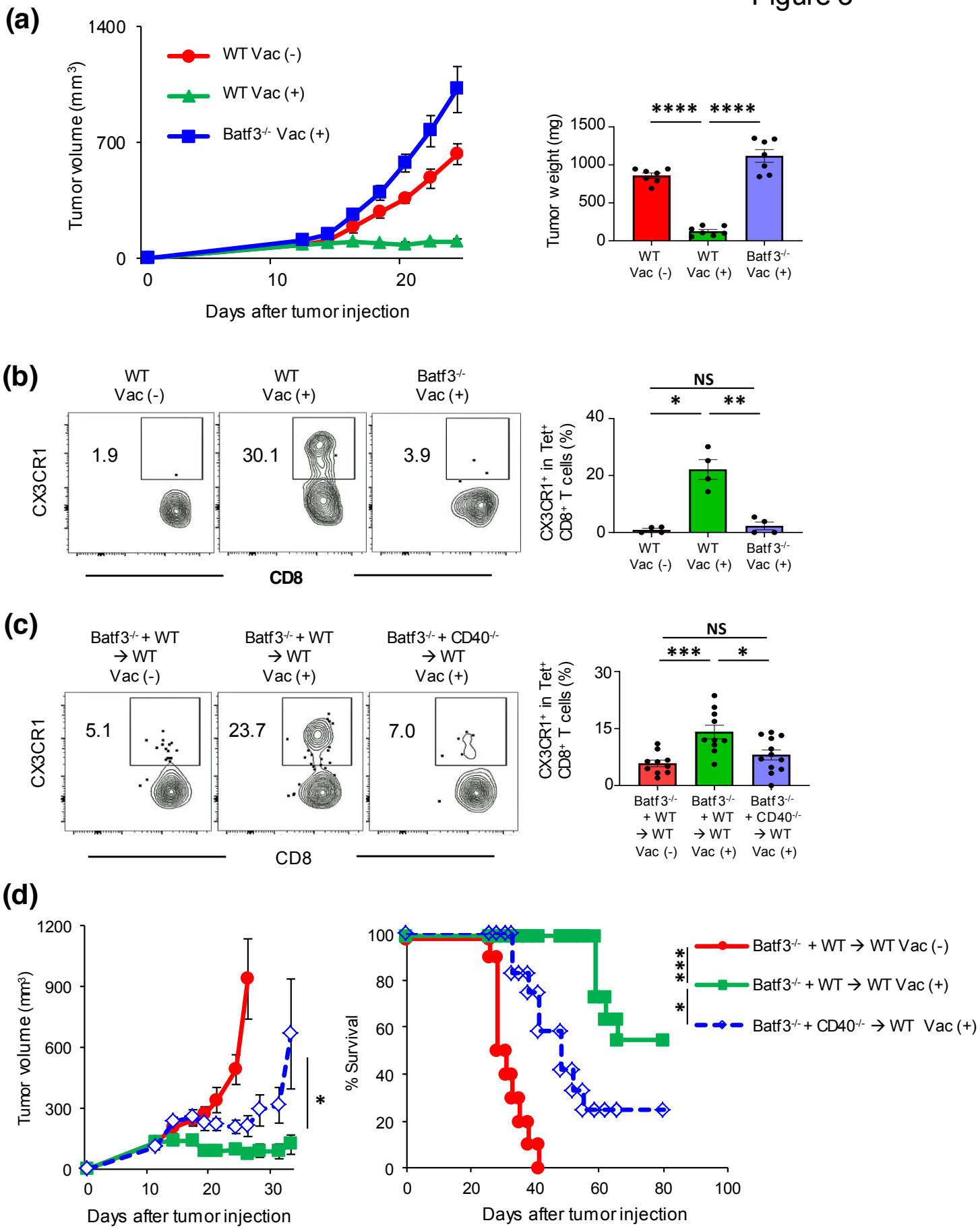
(a)
1400
700
0
Tumor volume (mm3)
WT Vac (-)
WT Vac (+)
Batf3-/- Vac (+)
0
10
20
Days after tumor injection
****
****
1500
1000
500
0
Tumor weight (mg)
WT Vac (-)
WT Vac (+)
Batf3-/- Vac (+)
(b)
WT Vac (-)
WT Vac (+)
Batf3-/- Vac (+)
CX3CR1
1.9
30.1
3.9
CD8
NS
*
**
40
20
0
CX3CR1+ in Tet++ CD8+ T cells (%)
WT Vac (-)
WT Vac (+)
Batf3-/- Vac (+)
(c)
Batf3-/- + WT → WT Vac (-)
Batf3-/- + WT → WT Vac (+)
Batf3-/- + CD40-/- → WT Vac (+)
CX3CR1
5.1
23.7
7.0
CD8
NS
***
*
30
15
0
CX3CR1+ in Tet++ CD8+ T cells (%)
Batf3-/- + WT → WT Vac (-)
Batf3-/- + WT → WT Vac (+)
Batf3-/- + CD40-/- → WT Vac (+)
(d)
1200
900
600
300
0
Tumor volume (mm3)
0
10
20
30
Days after tumor injection
*
100
80
60
40
20
0
% Survival
0
20
40
60
80
100
Days after tumor injection
***
*
Batf3-/- + WT → WT Vac (-)
Batf3-/- + WT → WT Vac (+)
Batf3-/- + CD40-/- → WT Vac (+)

Figure 5. Critical roles of CD40 signaling in cDC1s for antitumor efficacy of neoantigen/TLR3/CD40 agonists vaccination and generation of antigen-specific $CX3CR1^{+}CD8^{+}$ T cells.

(**a**) Left shows tumor volume curves in MC38 tumor-bearing wild type C57BL/6 mice (WT) or $Batf3^{-/-}$ mice treated with or without $Adpgk^{Mut}$/TLR3/CD40 agonists vaccination (Vac) (n = 7 mice per group). Tumors were harvested 1 week after second Vac, and tumor weight (mg) is shown in the right panel.

(**b**) Left shows representative FACS plots showing CD8 and CX3CR1 expression gated with PB $Adpgk^{Mut}$ $Tet^{+}CD8^{+}$ T cells in MC38 tumor-bearing WT or $Batf3^{-/-}$ mice treated with or without Vac. Numbers denote percentage of the $CX3CR1^{+}$ subset. Right shows the frequency of the $CX3CR1^{+}$ subset in each group (n = 4 mice per group).

(**c**) Left shows representative FACS plots showing CD8 and CX3CR1 expression gated with $Adpgk^{Mut}$ Tet^{+} $CD8^{+}$ T cells in PB of MC38-tumor bearing bone marrow chimera mice ($Batf3^{-/-}$ and WT→WT or $Batf3^{-/-}$ and $CD40^{-/-}$→WT mice) treated with or without Vac. PB was harvested 1 week after second Vac (**b** and **c**). Data shown are representative of two independent experiments (**a**, **b** and **c**).

(**d**) Tumor growth and survival curves in MC38 tumor-bearing mixed bone marrow chimera mice ($Batf3^{-/-}$ and WT→WT or $Batf3^{-/-}$ and $CD40^{-/-}$→WT mice) treated with or without Vac (n = 10-11 mice per group). Data shown are pooled from two independent experiments. $*P < 0.05$, $**P < 0.01$, $***P < 0.001$, $****P < 0.0001$ by one-way ANOVA with Tukey's multiple comparisons (**a**, **b** and **c**), Mann-Whitney *U* test (**d** for tumor volume), or log-rank (Mantel-Cox) test (d for survival). Mean ± SEM.

Figure 6

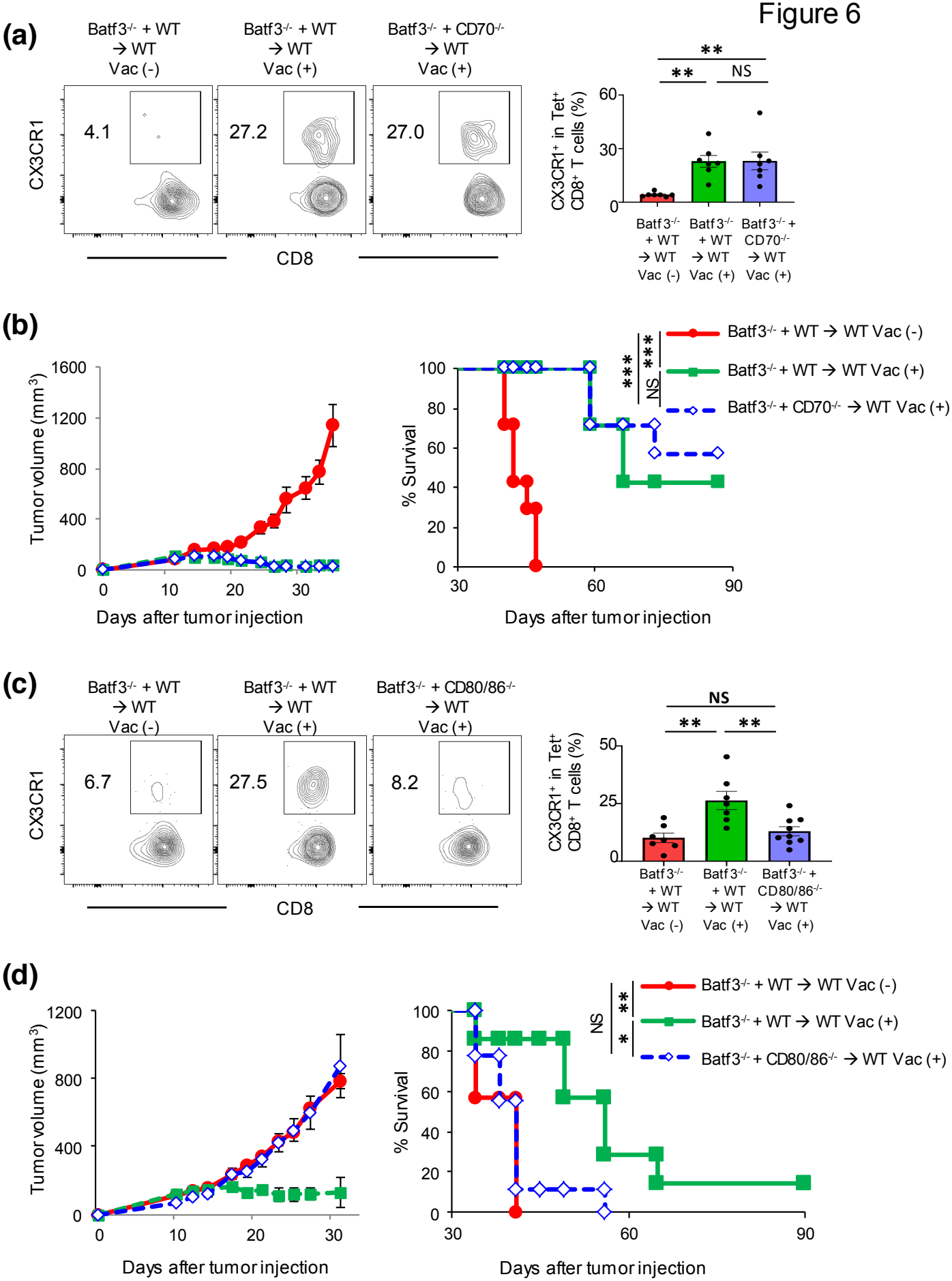
(a)
Batf3-/- + WT → WT Vac (-)
Batf3-/- + WT → WT Vac (+)
Batf3-/- + CD70-/- → WT Vac (+)
CX3CR1
CD8
4.1
27.2
27.0
CX3CR1+ in Tet+ CD8+ T cells (%)
**
**
NS
(b)
Tumor volume (mm3)
Days after tumor injection
% Survival
***
***
NS
Batf3-/- + WT → WT Vac (-)
Batf3-/- + WT → WT Vac (+)
Batf3-/- + CD70-/- → WT Vac (+)
(c)
Batf3-/- + CD80/86-/- → WT Vac (+)
6.7
27.5
8.2
NS
(d)
Batf3-/- + CD80/86-/- → WT Vac (+)
*

Figure 6. Roles of CD80/86 and CD70 signaling in cDC1s for antitumor efficacy of neoantigen/TLR3/CD40 agonists vaccination and generation of antigen-specific CX3CR1^{+}CD8^{+} T cells.

(**a**) Left shows representative FACS plots showing CD8 and CX3CR1 expression gated with Adpgk^{Mut} Tet^{+} CD8^{+} T cells in PB of MC38-tumor bearing bone marrow chimera mice (Batf3$^{-/-}$ and WT→WT or Batf3$^{-/-}$ and CD70$^{-/-}$→WT mice) treated with or without Adpgk^{Mut}/TLR3/CD40 agonists vaccination (Vac) Right shows the frequency of the CX3CR1^{+}Tet^{+}CD8^{+} T cells in each group (n = 7 mice per group).

(**b**) Tumor growth and survival curves of MC38 tumor-bearing mixed bone marrow chimera mice in different treatment groups as indicated. (n = 7 mice per group)

(**c**) Left shows representative FACS plots showing CD8 and CX3CR1 expression gated with Adpgk^{Mut} Tet^{+} CD8^{+} T cells in PB of MC38-tumor bearing bone marrow chimera mice (Batf3$^{-/-}$ and WT→WT or Batf3$^{-/-}$ and CD80/86$^{-/-}$→WT mice) treated with or without Vac (n = 7-9 mice per group).

(**d**) Tumor growth and survival curves of MC38 tumor-bearing mixed bone marrow chimera mice in different treatment groups as indicated (n = 7-9 mice per group).

PB was harvested 1 week after second Vac (**a** and **c**). Data shown are representative from two or three independent experiments. NS not significant, $*P<0.05$, $**P<0.01$, $***P<0.001$ by one-way ANOVA with Tukey's multiple comparisons (**a**, **c**) or log-rank (Mantel-Cox) test (**b**, **d**). Mean ± SEM.

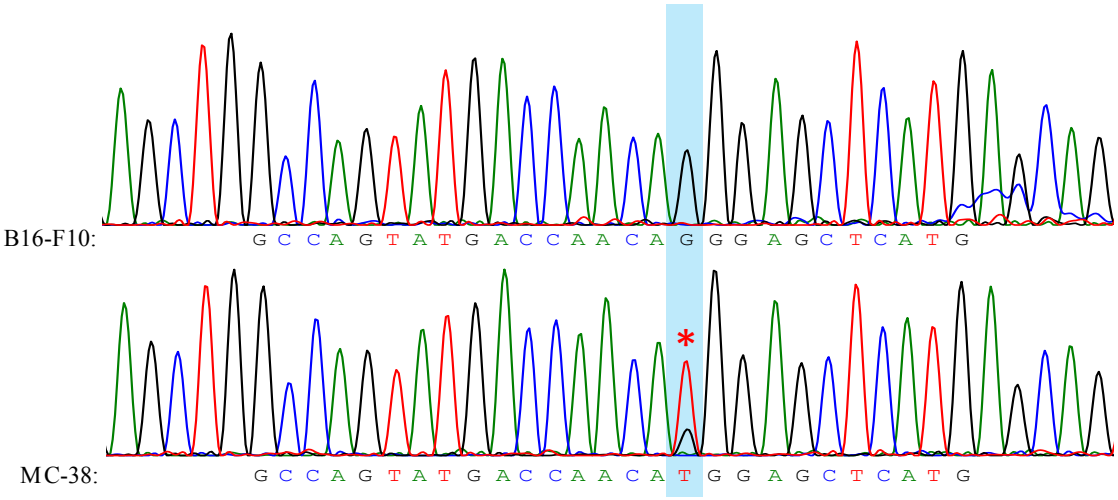

Supplementary Figure 1 cDNA sequencing of mutated Adpgk neoantigen in MC38 cells

Total RNA was extracted from MC38 cells (harboring mutated Adpgk) along with B16F10 cells (harboring wild type Adpgk), and subjected to cDNA synthesis for Sanger DNA sequencing. An asterisk indicates the mutation of G→T, resulting in arginine (R) to methionine (M) transformation on 304th amino acid sequences of Adpgk gene.

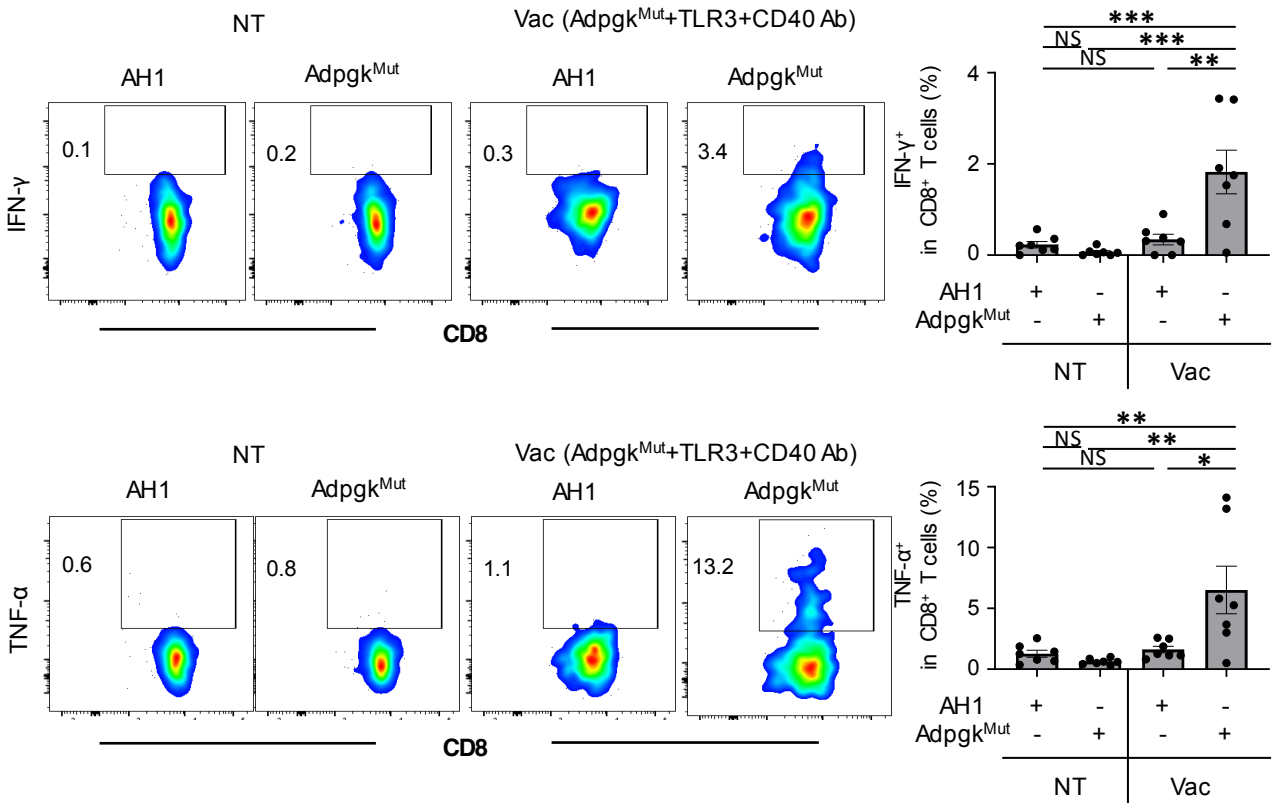

Supplementary Figure 2 Neoantigen/TLR3/CD40 vaccination facilitates neoantigen-specific CD8⁺ T cell infiltration into tumors

Left shows representative FACS plots showing CD8 and IFN-γ (upper) or TNF-α (lower) expression gated with CD8⁺ T cells in tumors of MC38-tumor bearing mice treated with PBS (NT) or neoantigen/TLR3/CD40 vaccinations. Tumor cells were co-cultured with AH1 or Adpgk peptide in the presence of blefeldin A for 5 hrs before intracellular staining. Numbers denote percentage of IFN-γ⁺ or TNF-α⁺ cells. Right panel shows the frequency of the IFN-γ⁺ cells in CD8⁺ T cells in each group (n = 7 mice per group). Data shown are representative from two or three independent experiments. NS not significant, *$P < 0.05$, **$P < 0.01$, ***$P < 0.001$ by one-way ANOVA with Tukey's multiple comparisons. Mean ± SEM.

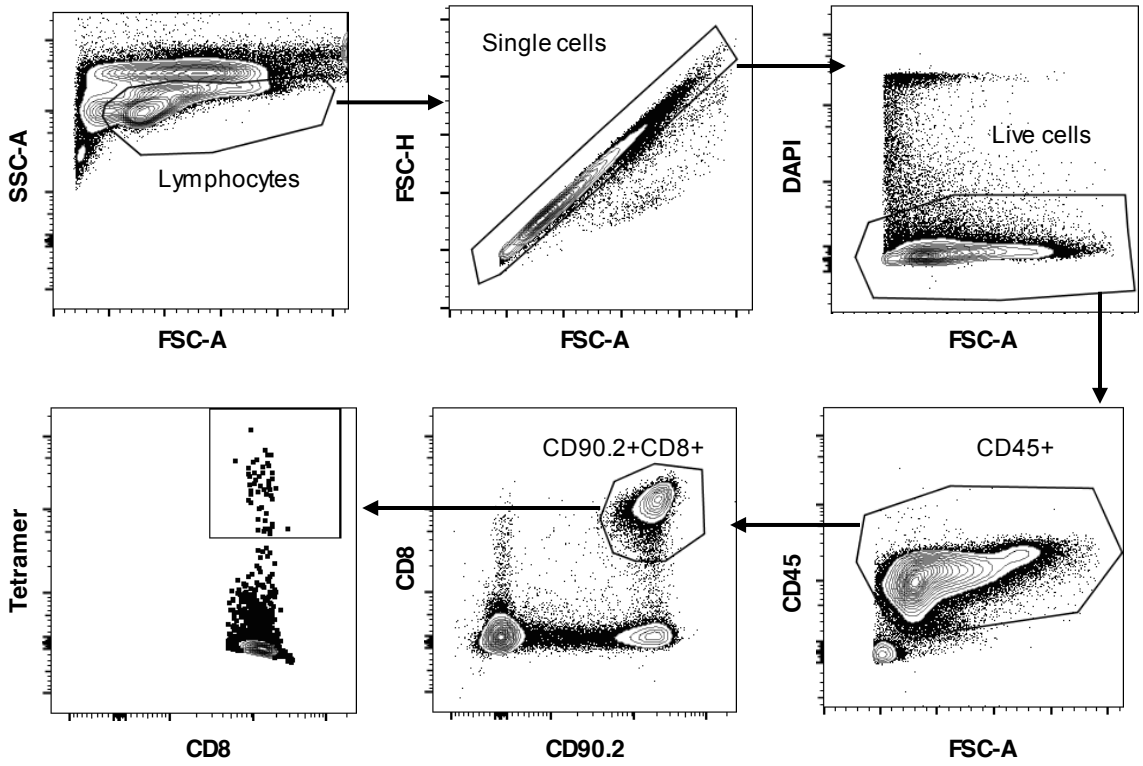

Supplementary Figure 3 Flow cytometry and gating of circulating Adpgk^{Mut} neoantigen-specific CD8^{+} T cells in MC38-tumor bearing mice. Representative of greater than 5 independent experiments.

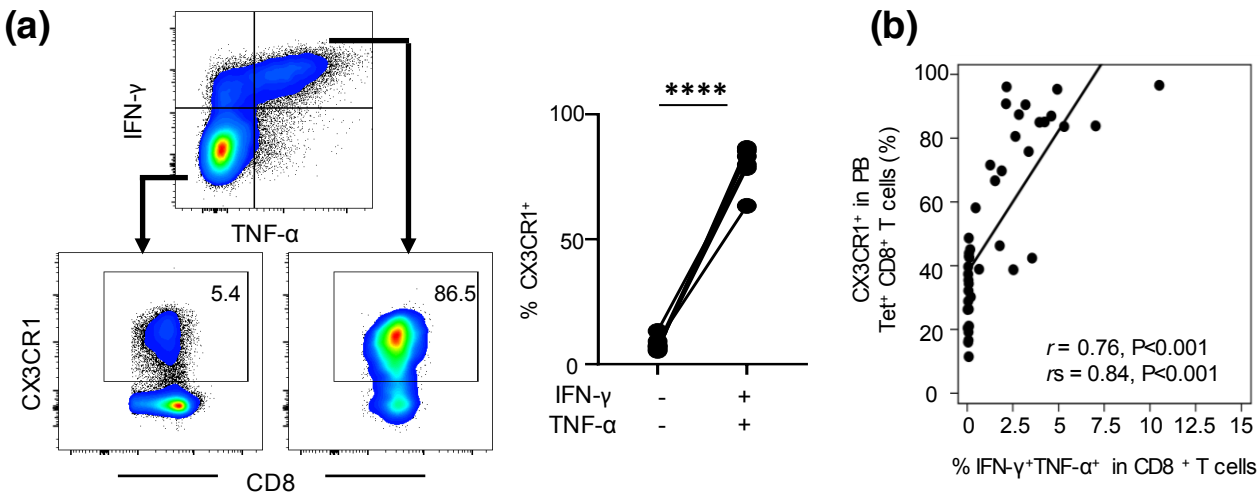

Supplementary Figure 4. High frequency of CX3CR1$^+$subset in neoantigen/TLR3/CD40 vaccination-induced peripheral CD8$^+$ T cells that are capable of producing effector cytokines.

(**a**) Representative FACS plots showing IFN-γ and TNF-α expression gated with CD8$^+$ T cells in splenocytes of MC38-tumor bearing mice treated with Adpgk^{Mut}/TLR3/CD40 vaccinations. Lower panels show CX3CR1 expression in IFN-γ$^-$ TNF-α$^-$ cells (left) and IFN-γ$^+$ TNF-α$^+$ cells (right). Numbers denote percentage of CX3CR1$^+$ cells. Data shown are representative of three independent experiments. Frequency of CX3CR1 cells from the IFN-γ$^-$ TNF-α$^-$ or IFN-γ$^+$ TNF-α$^+$ subset is shown in the right panel (n = 7 mice per group). Spleens were harvested 1 week after second vaccination. **** $P < 0.0001$ by paired two-tailed *t*-test (**a**).
(**b**) Scatter plot of the frequency of IFN-γ$^+$TNF-α$^+$ cells against the frequency of Adpgk^{Mut} tetramer (Tet)$^+$ CX3CR1$^+$CD8$^+$ T cells in splenocytes. Correlation is shown using Pearson correlation (r) and Spearman correlation coefficients (r_s).
Data shown are representative of two independent experiments.

Table S1: Fluorochrome-conjugated antibodies used in flow cytometry

Antibody	Clone	Manufacturer
CD8	53-6.7	Biolegend
CD90.1	OX-7	BioLegend
CD90.2	53-2.1	BioLegend
CX3CR1	SA011F11	BioLegend
CD45	30-F11	BD Biosciences
CD62L	MEL-14	Biolegend
4-1BB	17B5	BioLegend
KLRG1	2F1	BD Biosciences
CXCR3	CXCR3-173	Biolegend
PD-1	29F.1A12	Biolegend
Granzyme A	GzA-3G8.5	Thermofisher
IFN-γ	XMG1.2	BD Biosciences
TNF-α	MP6-XT22	Biolegend